Desalination and Water Treatment
www.deswater.com
51 (2013) 2317–2326
February
Taylor & Francis
Taylor & Francis Group
1944-3994/1944-3986 © 2013 Balaban Desalination Publications. All rights reserved
doi: 10.1080/19443994.2012.734585

Adsorption characteristics of silver ions onto activated carbon prepared from almond shell

Abdessalem Omri*, Mourad Benzina

Laboratory of Water-Energy-Environment (LR3E), code: AD-10-02, National School of Engineers of Sfax, University of Sfax, BP W, 3038 Sfax, Tunisia
Tel. +216 96803179; email: omriabdesslem@yahoo.fr

Received 26 January 2012; Accepted 26 July 2012

ABSTRACT

The adsorption of Ag(I) ions from aqueous solutions by almond shell activated carbon (ASC) was studied in a batch adsorption system. The BET surface area, total pore volume, and mesopore volume of ASC produce were found to be 893.62 m^2/g, 0.472, and 0.293 cm^3/g, respectively. Factors influencing Ag adsorption such as initial Ag ion concentration (170–680 mg/l), pH (2–12), contact time (10–180 min), and temperature (298–308 K) were investigated. The adsorption process was relatively fast and equilibrium was established about 60 min. Maximum adsorption of Ag(I) ions occurred at around pH 4.5. A comparison of the kinetic models on the overall adsorption rate showed that the adsorption system was best described by the pseudo second-order kinetics. The adsorption equilibrium data fitted best with the Langmuir isotherm and the monolayer adsorption capacity of Ag(I) ions was determined as 59.52 mg/g at 308 K. Thermodynamic parameters were calculated for the Ag(I) ion–ASC system and the positive value of ΔH (28.446 kJ/mol) showed that the adsorption was endothermic and physical in nature.

Keywords: Almond shell; Activated carbon; Silver; Adsorption isotherm; Kinetic; Thermodynamic

1. Introduction

Silver (Ag) is considered of special economic interest compared with other metals. Silver nitrate is the most common soluble salt that is used in porcelain, mirroring, photography, electroplating, and ink formulation industries [1]. This metal is a very useful raw material in various industries due to its excellent malleability, ductility, electrical and thermal conductivity, photosensitivity, and antimicrobial properties [2]. Significant amounts of Ag are lost in the effluents discharged from such industries and due to the toxicity of Ag to living organisms, the removal of this metal from wastewaters is an important concern. A number of adsorbents have been developed and tested for the removal and recovery of Ag(I) (e.g. activated carbon [3,4], cellulose nitrate membrane [5], and chelating resins [6]). Many studies have appeared on the development of low-cost activated carbon adsorbents produced from cheaper and readily available materials in the literature [7,8]. Activated carbons with their large surface area, microporous character, and chemical nature of their surface have made them potential adsorbents for the removal of heavy metals from industrial wastewater. Therefore, in recent years, many researchers have tried to produce activated carbons for removal of various pollutants using renewable and cheaper precursors which were mainly industrial and agricultural by-products, such as

*Corresponding author.

coconut shell [9], waste apricot [10], palm shell [11], molasses [12], rubber wood sawdust [13], rice straw [14], bamboo [15], sugarcane bagasse pith [16], oil palm fiber [17], and coconut husk [18].

This study reports the use of almond shell activated carbon (ASC), produced by pyrolysis and physical activation in the presence of water vapor, as an adsorbent to remove off Ag(I) ions from synthetic solution of silver nitrate regarded as a model of radiological effluent. At present, this almond shell material is used principally as a solid fuel and is available in abundance in Sfax, Tunisia. The production of almond shell is estimated to exceed 60,000 t/year.

In this study, the experimental parameters for the adsorption of Ag(I) ions from aqueous solutions under different equilibrium conditions were investigated in a batch study. The equilibrium isotherm data were treated with four adsorption isotherm models, Langmuir, Freundlich, Dubinin–Radushkevich, and Harkins–Jura. Values of kinetics studies of Ag(I) have been reported. In addition to this, characterization of ASC was studied in terms of surface area, surface morphology, and surface chemical.

2. Experimental procedure

2.1. Materials

Almond shell was collected from a company "Chaabane" located in Sfax, Tunisia. Silver nitrate (Merck, >99% purity) was used as a source of Ag(I).

2.2. Adsorbent preparation

The starting material was cleaned with water and dried at 110°C for 48 h. The dried sample was crushed with a blender and sieved to desired mesh size (1–2 mm). Activated carbons were prepared from almond shell by carbonization under nitrogen (N_2) flow and activation under water vapor. Carbonization was carried in a vertical stainless steel reactor (length 170 mm, interior diameter 22 mm) which was inserted into a cylindrical electric furnace Nabertherm. Almond shells were placed into the reactor and heated from room temperature to 400°C at a constant heating rate of 10°C/min under N_2 flow, then were held at 400°C for 1 h. The samples were left to cool down after the carbonization. Activation was carried out in the same furnace. The charcoal obtained was then physically activated at 850°C for 2 h under a N_2 flow (100 cm^3/min) saturated in steam after passing through the water saturator heated at 80°C. The tenor steam was fixed to 0.395 kg H_2O/kg N_2. After activation, the sample was cooled to ambient temperature under N_2 flow rate. The produced activated carbon was then dried at 105°C overnight, ground, and sifted to obtain a powder with a particle size smaller than 45 μm, and finally kept in hermetic bottle for subsequent uses.

2.3. Physico-chemical characteristics of the activated carbon

2.3.1. Textural characterization

The microstructure of the prepared activated carbon was examined using a scanning electron microscopy (SEM, Philips XL30 microscope). The specific surface area (S_{BET}) is determined by the adsorption of N_2 by using an apparatus BET of the type "ASAP 2010".

2.3.2. Chemical characterization

The surface organic functional groups and structure were studied by a Fourier transform infrared spectrometer (FTIR). The FTIR spectra of the resulting activated carbon were recorded between 500 and 4,000 cm^{-1} in a NICOET spectrometer.

The well-known Boehm's method allows modeling the principal acidic oxygenated functions of the activated carbon such as carboxylic acids, lactones, and phenols using bases of increasing strength as $NaHCO_3$, Na_2CO_3 and NaOH, respectively. Then, the total basicity is given by titration by HCl. More details are given in [19,20].

The pH of the prepared adsorbent was determined as follows: 5.0 g of carbon is weighed into a 250 ml beaker and 100 ml of water is added. The beaker is heated to boiling temperature for 5 min. The decanted portion is cooled to room temperature and pH value is measured.

The point of zero charge (pH_{PZC}) characteristic of the ASC was determined by using the solid addition method [21].

2.4. Procedure for adsorption of silver (I): batch adsorption

The effects of experimental parameters such as, initial metal ion concentration (170–680 mg/l), pH (2–12), and temperature (25–35°C) on the efficiency adsorption of Ag(I) ions were studied in a batch mode of operation for a specific period of contact time (10–180 min). The pH was adjusted using 0.1 N HCl or 0.1 N NaOH. The Ag(I) solutions were prepared by dissolving silver nitrate in double distilled water. For kinetic studies, 50 mL of Ag(I) solution of known initial concentration was taken in a 250 ml screw capconical flask with a fixed adsorbent dosage (0.1 g) and

was agitated in a thermostated rotary shaker for a contact time varied in the range (10–180 min) at a speed of 200 rpm. At various time intervals, the adsorbent was separated from the samples by filtering through polytetrafluoroethylene syringe filters (pore size: 0.45 μm) and the filtrate was analyzed using a ZEENIT atomic absorption. The amount of adsorption at equilibrium, q_e (mg/g), and the adsorption percentage, % adsorption, were calculated by the following equations:

$$Q_e = \frac{(C_0 - C_e)V}{m} \quad (1)$$

$$\% \text{ Absorption} = \frac{C_0 - C_e}{C_0} \times 100 \quad (2)$$

where C_0 and C_e (mg/l) are the liquid-phase concentrations of Ag(I) initially and at equilibrium, respectively. V is the volume of the solution (l) and m is the mass of dry adsorbent used (g). Adsorption isotherms were obtained by plotting adsorption capacities with respect to equilibrium concentrations.

3. Results and discussion

3.1. Characterization of ASC

3.1.1. SEM micrograph and surface area

The ASC has prepared the following textural characteristics: a BET surface area of 893.62 m^2/g, a total pore volume of 0.472 cm^3/g, and mesopore volume of 0.293 cm^3/g. This value of mesopore volume indicated that the ASC was in the mesoporous region. Comparing the surface area with that reported in the literature for others activated the carbons prepared from the same precursor in different activation conditions, the ASC has significant value of surface area (Table 1).

Table 1
Compared surface area of the ASC

Activation conditions		S_{BET} (m^2/g)	Reference
Activation agent	Temperature (°C)/ Time (h)		
H_3PO_4	450/1.0	822	[22]
CO_2	800/2.0	851	[23]
CO_2	800/3.0	1,012	[23]
H_2SO_4	200/24	412	[24]
Air	750/1.66	733	[25]
Steam	850/1.5	587	[26]
Steam	850/2.0	893	This work

The SEM micrograph of ASC samples are given in Fig. 1. The external surfaces of these prepared activated carbon show presence cavities and are very irregular, indicating that the porosity of the material was produced by attack of the reagent (H_2O) during activation [27].

The increase in the steam tenor supports the following gasification process under high temperature [28]:

$$H_2O + C \rightarrow H_2 + CO \quad (3)$$

After undergoing carbonization and activation process, the volatile matter content decreased significantly, whereas the fixed carbon content increased in ASC, this was due to the pyrolytic effect where most of the organic substances have been degraded and discharged as gas and liquid tars leaving a material with high carbon purity [29]. Adinata et al. [30] found that increasing the carbonization temperature decreased the yield progressively due to the release of volatile products as a result of intensifying dehydration and elimination reaction.

3.1.2. IR spectra

The FTIR spectrum of ASC is illustrated in Fig. 2. The bands at 3,440 and 1,088 cm^{-1} were assigned to O–H bonds and C–OH stretching of phenolic groups, respectively [31]. Aliphatic C–H stretching vibration is found as a very weak peak at 2,884 cm^{-1} while asymmetric vibration of CH_2 group appears at 2,920 cm^{-1}. The bands located at about 1,620 and 1,395 cm^{-1} were attributed to carbonyl (e.g. ketone) and carboxylate ion (COO^-) groups, respectively.

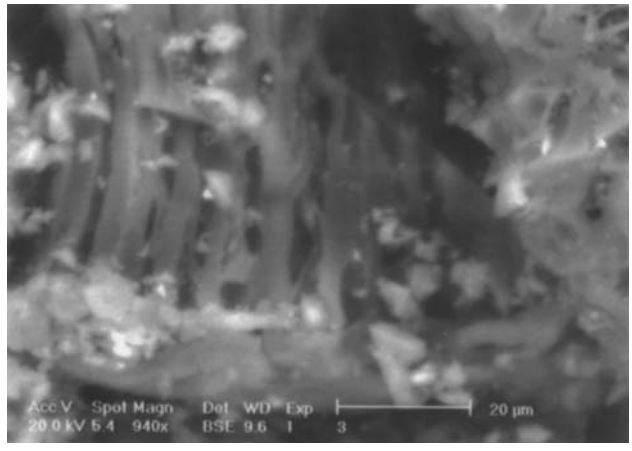

Fig. 1. SEM image of ASC.

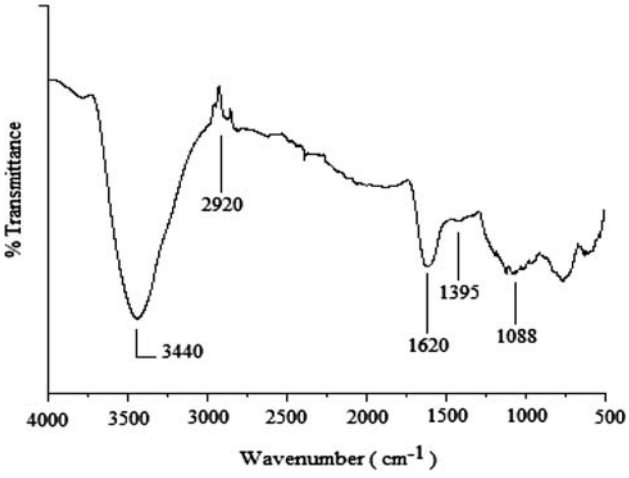

Fig. 2. FTIR spectrum of the ASC.

3.1.3. Oxygen functional groups

The identification and quantification of the surface oxygen groups in the prepared carbon was done by means of the point of zero charge and Boehm titration. The results are shown in Table 2. Acidic surface groups consist of temperature-sensitive and temperature-insensitive types. Temperature-sensitive types of acidic surface groups can decompose at high temperature. Therefore, high activation temperature favors low acidity [32]. Hence, activated carbons produced by physical activation are basic character in general. For this reason, the activated carbon prepared has predominantly basic surface groups. On the other hand, the carbon also possesses high ash content; therefore, the basic nature might also be associated to the mineral matter of the carbon (Lewis basic structures). This unusual characteristic has also been reported for activated carbons obtained from other lingo-cellulosic precursors such as cork powder [33,34]. The pH of the activated carbon was measured as 9.16. This result confirmed the Boehm analysis.

Table 2
Chemical parameters of the ASC obtained from Boehm method, pH, and point of zero charge.

Chemical parameters	Values
Total of acid functions	1.708
Carboxylic (–COOH)	1.390
Lactones (–COO–)	0.172
Phenol (–OH)	0.146
Total of basic functions	4.905
pH	9.16
pH_{PZC}	8.62

3.2. Effect of pH on adsorption of Ag(I) onto the ASC

It is well known that pH of the solution is a critical factor in adsorption from solution; not only carbon surface properties change with variations of the pH, but this parameter can also affect the state of the ionic species in solution. The effect of pH on Ag(I) adsorption was studied in the initial pH range between 2 and 12, at a contact time of 60 min (Fig. 3). The removal of Ag(I) increases with the pH of the system, and it reaches a maximum around 4.5 pH units. At pH above this value, a slight decrease until pH 8 and then a sharp decrease is obtained in the uptake of Ag(I). This decreased adsorption of Ag(I) prior to initial pH 8 may be due to the masking of Ag(I) ions in the form of soluble hydroxide anions. At pH > 8, almost all of the Ag (I) ions are precipitated in the form of AgOH [35]. The effect is particularly more remarkable at pH 12, being the amount adsorbed very low, close to 63.01 mg/g. According to data shown in Table 1, the pH_{PZC} of a carbon is 8.62. At low pH (acidic) of the solution the carbon surface is predominantly positively charged, whereas at strong basic pH above the pH_{PZC}, negative charges appear on the surface (reduction of the number of protons H^+). So, increased external H^+ concentration (due to lowered pH) may have effected Ag ion removal via ion exchange by direct competition effects between the protons and Ag ions for the exchange sites on the activated carbon. This result can be considered as an evidence for the Ag ion removal via ion exchange mechanism in this study.

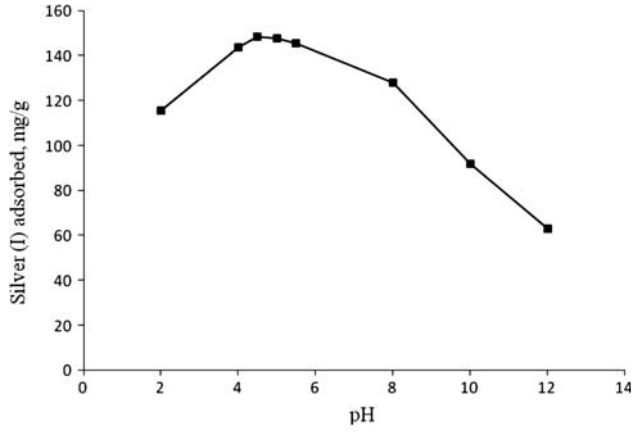

Fig. 3. Effect of initial concentration on the adsorption of Ag(I) by ASC at 298 K, time = 60 min and Ag(I) initial concentration = 510 mg/l.

The adsorption mechanism of Ag ions onto prepared activated carbon can be represented according to the following reaction:

$$\underset{\text{Activated carbon}}{(\text{ASC–OH})} + Ag^{+} \rightarrow \underset{\text{Activated carbon–Ag}}{(\text{ASC–O})Ag} + H^{+} \quad (4)$$

3.3. Effect of initial silver concentration and contact time

The kinetics of Ag(I) sorption was studied by varying the contact time from 10 to 180 min using different initial Ag concentrations (170, 340, 510, and 680 mg/l), various temperatures (298, 308, and 318 K), and fixed the value of pH to 4.5.

The amount of Ag adsorbed for different initial concentrations onto ASC is shown in Fig. 4.

The adsorption of Ag(I) onto ASC increases with time and then attains equilibrium value at a time of about 60 min. The removal of Ag(I) was found to be dependent on the initial concentration; the amount adsorbed increasing with increase in initial concentration. Further, the adsorption is rapid in the early stages and then attains an asymptotic value for larger adsorption time. At low concentrations, the ratio of available surface to the initial Ag(I) concentration is larger, so the removal becomes independent of initial concentrations. However, in the case of higher concentrations this ratio is low; the percentage removal then depends upon the initial concentration. On changing the initial concentration from 170 to 680 mg/l, the amount adsorbed increased from 23.4371 to 159.375 mg/g for a time period of 60 min.

3.4. Effect of solution temperature

Adsorption experiments were conducted at 298, 303, and 308 K to investigate the effect of temperature, with initial Ag(I) concentration of 42.5–255 mg/l, contact time of 60 min, and fixed the value of pH to 4.5 (Fig. 5).

It was observed that the maximum adsorption of Ag(I) ion increased from 80% at 298 K to 87.56% at 308 K, i.e. adsorption increased with the increase of temperature (Fig. 5). This can be explained by the fact that at higher temperature, the kinetic energy of Ag(I) cations is high; therefore, contact between Ag(I) and the active sites of ASC is sufficient, leading to an increase in adsorption efficiency.

This condition shows that adsorption is more of a physical than a chemical adsorption. Similar trends are also observed by other researchers for aqueous-phase adsorption [36]. In addition to that, the rise of adsorption with temperature may enlarge the pore size to some extent which may also affect the carbon adsorption capacity.

3.5. Adsorption isotherms

Adsorption isotherms are important in predictive modeling the procedures for designing the adsorption system, because the adsorption capacity of a quantitative of adsorbent could be described, making the selection of appropriate adsorbent and determination of adsorbent dosage feasible [37]. In our equilibrium experiments, the initial Ag(I) concentrations varying from 42.5 to 255 mg/l have been involved and the experiments were conducted under the conditions that the carbon dose and pH value were 0.1 g and 4.5 and also at various temperature (298, 303, and 308 K), then the widely used Langmuir isotherm [38], Freundlich isotherm [39], Dubinin–Radushkevich isotherm [40], and Harkins–Jura isotherm [41] were applied to analyze experimental data.

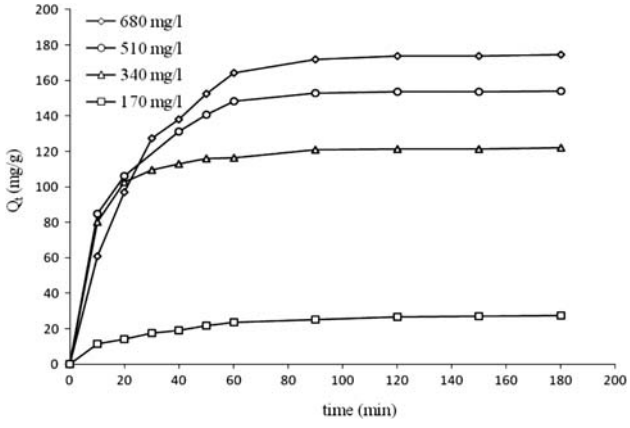

Fig. 4. Effect of initial concentration on the adsorption of Ag(I) by ASC at 298 K and pH = 4.5.

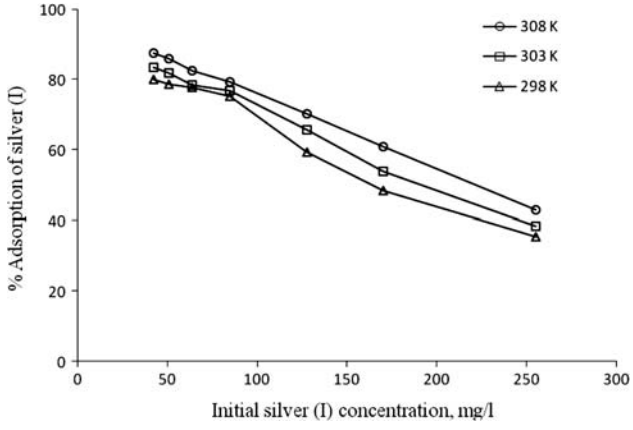

Fig. 5. Effect of temperature on the adsorption of Ag(I) by ASC at time = 60 min and pH = 4.5.

The linear form of Langmuir isotherm equation is given as:

$$\frac{C_e}{q_e} = \frac{1}{Q_m b} + \frac{C_e}{Q_m} \tag{5}$$

where C_e is the equilibrium concentration of the adsorbate (mg/l), q_e is the amount of adsorbate adsorbed per unit mass of adsorbent (mg/g), b the Langmuir adsorption constant (l/mg), and Q_m is the theoretical maximum adsorption capacity (mg/g). A straight line with slope of $1/Q_m$ and intercept of $1/Q_m b$ is obtained when C_e/q_e is plotted against C_e (Fig. 6).

Freundlich model is based on sorption on a heterogeneous surface of varied affinities. The logarithmic form of Freundlich was given as:

$$\log q_e = \log K_F + \left(\frac{1}{n}\right) \log C_e \tag{6}$$

where K_F and n are Freundlich constants with n as a measure of the deviation of the model from linearity of the adsorption and K_F (mg/g(l/mg)$^{1/n}$) indicates the adsorption capacity of the adsorbent. In general, n>1 suggests that adsorbate is favorably adsorbed on the adsorbent. The higher the $1/n$ value the stronger the adsorption intensity. The plot of log q_e versus log C_e gave a straight line with slope of $1/n$ and intercept of log K_F (Fig. 7).

The linear form of Dubinin–Radushkevich isotherm equation can be expressed as

$$\text{In } q_e = \text{In } Q_s - B\varepsilon^2 \tag{7}$$

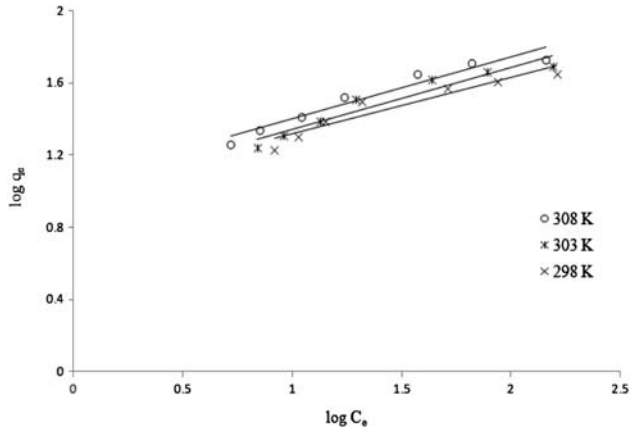

Fig. 7. Freundlich isotherm for adsorption of Ag(I) onto ASC at different temperatures. (temperature = 298, 303, and 308 K; t = 60 min, pH = 4.5).

where Q_S is the theoretical monolayer saturation capacity (mg/g), B is the Dubinin–Radushkevich model constant (mol^2/kJ^2), and ε is the Polanyi potential and is equal to

$$\varepsilon = RT \ \text{In}\left(1 + \frac{1}{C_e}\right) \tag{8}$$

The mean energy of sorption, E (kJ/mol), is related to B as [42]

$$E = \frac{1}{\sqrt{2B}} \tag{9}$$

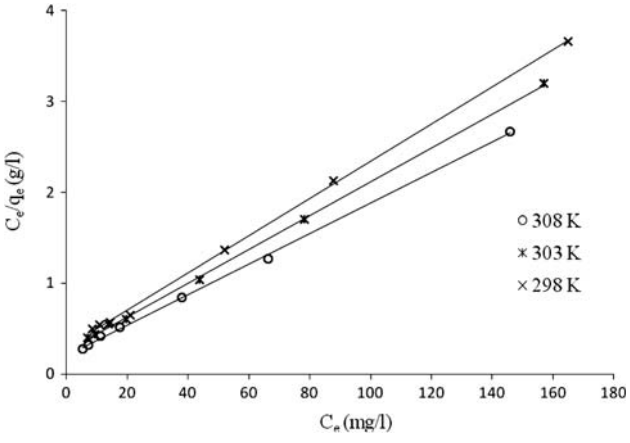

Fig. 6. Langmuir isotherm for adsorption of Ag(I) onto ASC at different temperatures. (temperature = 298, 303, and 308 K; t = 60 min, pH = 4.5).

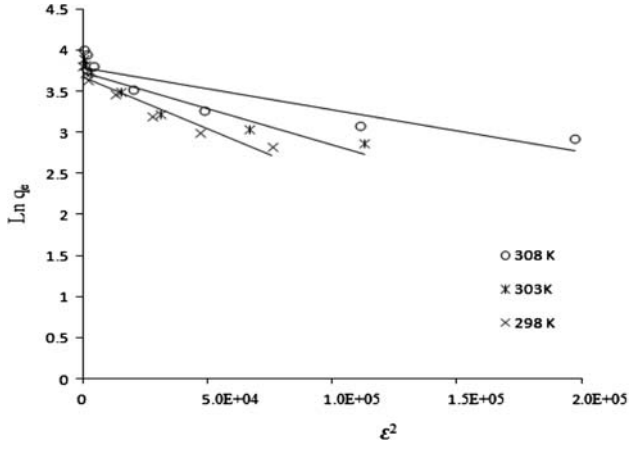

Fig. 8. Dubinin–Radushkevich isotherm for adsorption of Ag(I) onto ASC at different temperatures. (temperature = 298, 303, and 308 K; t = 60 min, pH = 4.5).

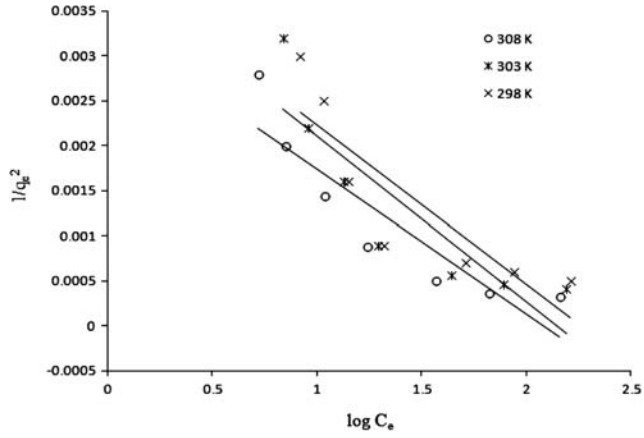

Fig. 9. Harkins–Jura isotherm for adsorption of Ag(I) onto ASC at different temperatures. (temperature = 298, 303, and 308 K; t = 60 min, pH = 4.5).

ln q_e vs. ε^2 was plotted at different temperatures as shown in Fig. 8.

The Harkins–Jura adsorption isotherm can be expressed as

$$\frac{1}{Q_e^2} = \left(\frac{B_2}{A}\right) - \left(\frac{1}{A}\right)\log C_e \quad (10)$$

where A and B_2 are the Harkins–Jura isotherm constant, which accounts to multilayer adsorption that can be explained with the existence of a heterogeneous pore distribution. $1/q^2$ vs. log C_e Harkins–Jura isotherms are given in Fig. 9.

The constants and correlation coefficient, R^2, values obtained from the two isotherm models applied for adsorption of Ag ions on the ASC were summarized in Table 3.

From Table 3, the values of n were found to be less than 10 indicating that the adsorption was favorable. The Langmuir isotherms were found to be linear over the whole temperature range studied and the correlation coefficients R^2 were extremely high compared to the Freundlich, Dubinin–Radushkevich, and Harkins–Jura isotherms, indicating that the Langmuir isotherm better represented the experimental adsorption data at all solution temperatures. As can be further seen from Table 3, the values of Q_m, K_F, and Q_s increased with temperature, indicating that the adsorption process was endothermic in nature.

3.6. Adsorption kinetics

In order to analyze the adsorption kinetics of Ag(I) ions onto ASC, two kinetic models; pseudo-first-order and pseudo-second-order kinetic were applied for the

Table 3
Langmuir, Freundlich, Dubinin–Radushkevich, and Harkins–Jura isotherms parameters for the adsorption of Ag(I) onto ASC at different temperatures and constant value of pH = 4.5

	Temperatures		
	298 K	303 K	308 K
Langmuir isotherm			
Q_m (mg/g)	48.78	53.76	59.52
b (l/mg)	0.069	0.072	0.082
R^2	0.998	0.999	0.999
Freundlich isotherm			
K_F (mg/g) (l/mg)$^{1/n}$	10.15	10.07	11.40
n	3.215	2.924	2.918
R^2	0.924	0.943	0.902
D–R isotherm			
Q_S (mg/g)	39.614	41.64	44.20
B × 10^6	0.1	9	5
E (kJ/mol)	2.23	2.35	3.16
R^2	0.934	0.866	0.808
Harkins–Jura isotherm			
A × 10^{-2}	5.55	5.55	6.25
B_2	2.22	2.22	2.06
R^2	0.756	0.769	0.817

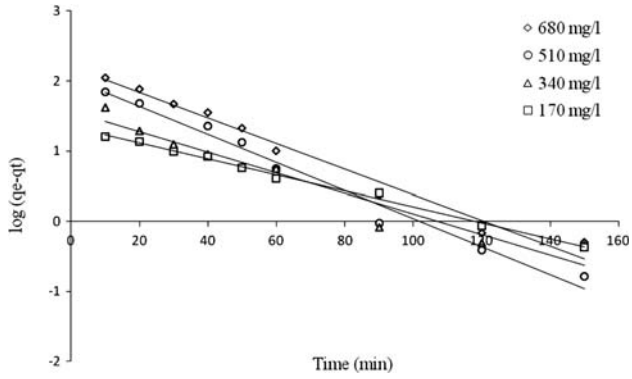

Fig. 10. Pseudo-first-order kinetic plot for the adsorption of Ag(I) onto ASC at 298 K and pH = 4.5.

experimental data. The pseudo-first-order equation can be expressed as [43]:

$$log(q_e - q_t) = log q_e - \frac{k_1}{2.303}t \quad (11)$$

where q_e and q_t are the amounts adsorbed at equilibrium and at time t (mg/g), and k_1 is the rate constant of the pseudo-first-order adsorption (min^{-1}). The linear plot of log ($q_e - q_t$) vs. t gives a slope of k_1 and intercept of log q_e as shown in Fig. 10.

Table 4
Pseudo-first-order and pseudo-second-order kinetic model parameters for the adsorption of Ag(I) onto ASC at 298 K and pH = 4.5

$[Ag^+]$ (mg/l)	q_e, exp (mg/g)	Pseudo-first-order			Pseudo-second-order		
		q_e, cal (mg/g)	K_1 (min^{-1})	R^2	q_e, cal (mg/g)	K_2 (g mg^{-1}min)	R^2
170	27.125	21.79	0.026	0.994	30.959	0.001	0.998
340	121.425	36.57	0.033	0.938	125	0.002	0.999
510	153.762	109.85	0.045	0.98	161.29	0.0008	0.999
680	173.875	158.7	0.042	0.97	192.307	0.0003	0.995

The values of k_1 and R^2 obtained from the plots for adsorption of Ag(I) ions on the adsorbent at 298 K are reported in Table 4. It was observed that the R^2 values obtained for the pseudo-first-order model did not show a consistent trend. Besides, the experimental q_e values did not agree with the calculated values obtained from the linear plots. This shows that the adsorption of Ag(I) on the adsorbent does not follow a pseudo first-order kinetic model.

The pseudo-second-order kinetic model can be represented in the following form [44]:

$$\frac{t}{q_t} = \frac{1}{k_2 q_e^2} + \frac{1}{q_e} t \tag{12}$$

where k_2 (g/mg min) is the rate constant of second-order adsorption. The linear plot of t/q_t vs. t gave $1/q_e$ as the slope and $1/k_2 {q_e}^2$ as the intercept as shown in Fig. 11.

From Table 4, all the R^2 values obtained from the pseudo-second-order model were close to unity, indicating that the adsorption of Ag(I) on ASC fitted well into this model.

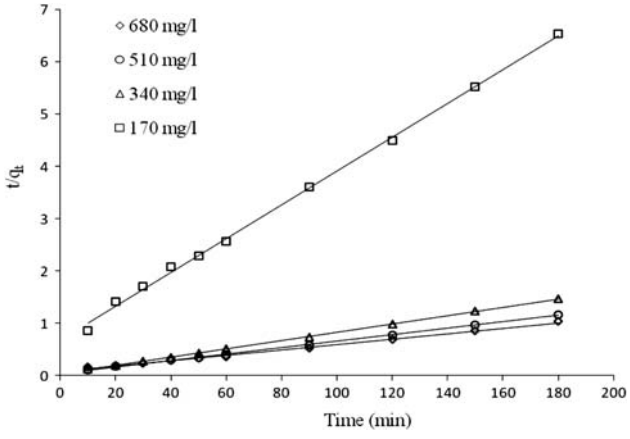

Fig. 11. Pseudo-second-order kinetic plot for the adsorption of Ag(I) onto ASC at 298 K and pH = 4.5.

Table 5
Thermodynamic parameters for the retention of Ag(I) onto ASC at different temperatures and pH = 4.5

Metal ion	Temperature (K)	ΔG (kJ/mol)	ΔS (kJ/mol K)	ΔH (kJ/mol)
Ag(I)	298	−3.005		
	303	−3.408	0.105	28.446
	308	−4.059		

3.7. Adsorption thermodynamics

The thermodynamic parameters for the present system, including standard free energy (ΔG, kJ/mol), enthalpy (ΔH, kJ/mol), and entropy (ΔS, kJ/mol K), were calculated using following equations Eqs. (13) and (14) [45]:

$$\Delta G = -RT\ln K \tag{13}$$

$$\Delta G = \Delta H - T\Delta S \tag{14}$$

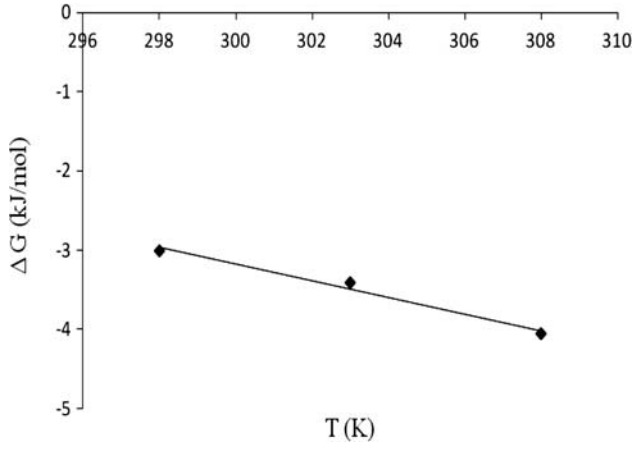

Fig. 12. Plot of ΔG vs. T for the estimation of thermodynamic parameters for adsorption of Ag(I) by ASC.

where T is the temperature (K), R is universal gas constant (8.314 J/mol K), and K (l/g) is an equilibrium constant obtained by multiplying the Langmuir constant Q_m and b. The K is the distribution constant characteristic of the equilibrium established between the Ag in solid and liquid phase [46]. The values of ΔH and ΔS were calculated from the intercept and slope of a plot of ΔG vs. T (Fig. 12) according to Eq. (14) by linear regression analysis.

The calculated thermodynamic parameters were listed in Table 5. As shown in Table 3, the positive value of ΔH indicates that the adsorption process is endothermic [47]. ΔG reflects the feasibility of the process and standard entropy determines the disorderliness of the adsorption at solid–liquid interface [48].

4. Conclusions

The ASC prepared by physical activation with steam was an efficient adsorbent with relative surface area of 893.62 m^2/g and mesopore volume of 0.293 cm^3/g. SEM and fourier transform infrared spectroscopy investigations were evidenced with the presence of a porous structure and different functionalities on the ASC surface. The present study shows that ASC could be used as an adsorbent for the removal of Ag from aqueous solutions. From batch experiments, the adsorption amount was highly dependent on operating variables such as initial metal concentration, pH, contact time, and temperature. The equilibrium time was found to be 60 min for Ag–ASC system and an acidic pH equal to 4.5. Efficiency adsorption increased with decreasing the metal concentration and increasing temperature. Experimental results indicated that the pseudo-second-order reaction kinetics provided the best description of the data. The isotherm study indicated that adsorption data correlated well with Langmuir isotherm model. Thermodynamical parameters were also evaluated for the metal ion adsorbent system and revealed that the adsorption was endothermic in nature. This study demonstrated that the ASC could be used as an effective adsorbent for the treatment of effluent from radiology.

Acknowledgments

Thanks are extended to Mr. Ibrahim Ben letaief, technician in Laboratory of Atomic Absorption, ENIS-Sfax for facilitating the analysis of samples using Atomic absorption spectrometer. We extend our thanks to Mr. Nidhal Baccar, technician in University of Sfax-Tunisia for his help and Mr. Hafedh Bejaoui for this linguistic assistance in this manuscript.

References

[1] J.W. Patterson, Industrial Wastewater Treatment, second ed., Butterworth, Boston, MA, 1985.
[2] M. Akgül, A. Karabakan, O. Acar, Y. Yüruüm, Removal of silver (I) from aqueous solutions with clinoptilolite, Micropor. Mesopor. Mater. 94 (2006) 99–104.
[3] M. Soylak, L. Elçi, M. Dogan, A sorbent extraction procedure for the preconcentration of gold, silver and palladium on an activated carbon column, Anal. Lett. 33 (2000) 513–525.
[4] M. Soylak, L. Elçi, I. Narin, M. Dogan, Separation/preconcentration of gold, silver and palladium from some aluminum and manganese salts on an activated carbon column, Asian J. Chem. 13 (2001) 699–703.
[5] M. Soylak, R.S. Çay, Separation/preconcentration of silver (I) and lead (II) in environmental samples on cellulose nitrate membrane filter prior to their flame atomic absorption spectrometric determinations, J. Hazard. Mater. 146 (2007) 142–147.
[6] H. Yirikoglu, M. Gülfen, Separation and recovery of silver (I) ions from base metal ions by melamine–formaldehyde–thiourea (MFT) chelating resin, Sep. Sci. Technol. 43 (2008) 376–388.
[7] S.E. Bailey, T.J. Olin, R.M. Bricka, D.D. Adrian, A review of potentially low-cost sorbents for heavy metals, Water Res. 33 (1999) 2469–2479.
[8] S.J.T. Pollard, G.F. Fowler, C.J. Sollars, R. Perry, Low cost adsorbents for waste and wastewater treatment: A review, Sci. Total Environ. 116 (1992) 31–52.
[9] M. Radhika, K. Palanivelu, Adsorptive removal of chlorophenols from aqueous solution by low cost adsorbent—kinetics and isotherm analysis, J. Hazard. Mater. B138 (2006) 116–124.
[10] C.A. Başar, Applicability of the various adsorption models of three dyes adsorption onto activated carbon prepared waste apricot, J. Hazard. Mater. B135 (2006) 232–241.
[11] G. Issabayeva, M.K. Aroua, N.M. Sulaiman, Study on palm shell activated carbon adsorption capacity to remove copper ions from aqueous solutions, Desalination 262 (2010) 94–98.
[12] K. Legrouri, E. Khouya, M. Ezzine, H. Hannache, R. Denoyel, R. Pallier, R. Naslain, Production of activated carbon from a new precursor molasses by activation with sulphuric acid, J. Hazard. Mater. B118 (2005) 259–263.
[13] B.G. Prakash Kumar, K. Shivakamy, Lima Rose Miranda, M. Velan, Preparation of steam activated carbon from rubberwood sawdust (*Hevea brasiliensis*) and its adsorption kinetics, J. Hazard. Mater. B136 (2006) 922–929.
[14] S.L. Wang, Y.M. Tzou, Y.H. Lu, G. Sheng, Removal of 3-chlorophenol from water using rice-straw-based carbon, J. Hazard. Mater. 147 (2007) 313–318.
[15] B.H. Hameed, A.T.M. Din, A.L. Ahmad, Adsorption of methylene blue onto bamboo-based activated carbon: Kinetics and equilibrium studies, J. Hazard. Mater. 141 (2007) 819–825.
[16] N.K. Amin, Removal of reactive dye from aqueous solutions by adsorption onto activated carbons prepared from sugarcane bagasse pith, Desalination 223 (2008) 152–161.
[17] I.A.W. Tan, B.H. Hameed, A.L. Ahmad, Equilibrium and kinetic studies on basic dye adsorption by oil palm fibre activated carbon, Chem. Eng. J. 127 (2007) 111–119.
[18] I.A.W. Tan, B.H. Hameed, A.L. Ahmad, Optimization of preparation conditions for activated carbons from coconut husk using response surface methodology, Chem. Eng. J. 137 (2008) 462–470.
[19] J. Starck, P. Burg, D. Cagniant, J.M.D Tascon, A. Martinez-Alonso, The effect of demineralisation on a lignite surface properties, Fuel 83 (2004) 845–850.
[20] H.P. Boehm, Some aspects of the surface chemistry of carbon blacks and other carbons, Carbon 32 (1994) 759–769.

[21] A. Kumar, B. Prasad, I.M. Mishra, Adsorptive removal of acrylonitrile by commercial grade activated carbon: Kinetics, equilibrium and thermodynamics, J. Hazard. Mater. 152 (2008) 589–600.
[22] C.A. Tolesa, W.E. Marshalla, M.M. Johnsa, L.H. Wartellea, A. McAloon, Acid-activated carbons from almond shells: Physical, chemical and adsorptive properties and estimated cost of production, Bioresour. Technol. 71 (2000) 87–92.
[23] J.M. Valente Nabais, C.E.C. Laginhas, P.J.M. Carrott, M.M.L. Ribeiro Carrott, Production of activated carbons from almond shell, Fuel Process. Technol. 92 (2011) 234–240.
[24] E. Demirbas, M. Kobya, A.E.S. Konukman, Error analysis of equilibrium studies for the almond shell activated carbon adsorption of Cr(VI) from aqueous solutions, J. Hazard. Mater. 154 (2008) 787–794.
[25] D. Mohana, A. Sarswata, V.K. Singha, M. Alexandre-Francob, Ch.U. Pittman Jr., Development of magnetic activated carbon from almond shells for trinitrophenol removal from water, Chem. Eng. J. 172 (2011) 1111–1125.
[26] K. Thomas Klasson, C.A. Ledbetter, L.H. Wartelle, Sarah E Lingle, Feasibility of dibromochloropropane (DBCP) and trichloroethylene (TCE) adsorption onto activated carbons made from nut shells of different almond varieties, Indus. Crops Prod. 31 (2010) 261–265.
[27] F. Rodriguez-Reinoso, J. Lopez-Gonzalez, D.de C. Berenguer, Activated carbons from almond shells-I preparation and characterization by nitrogen adsorption, Carbon 20 (1982) 513–518.
[28] I.A.W. Tan, A.L. Ahmad, B.H. Hameed, Preparation of activated carbon from coconut husk: Optimization study on removal of 2,4,6-trichlorophenol using response surface methodology, J. Hazard. Mater. 153 (2008) 709–717.
[29] M.A. Ahmad, W.M.A. Wan Daud, M.K. Aroua, CO_2/CH_4 and O_2/N_2 kinetic selectivities of oil palm shell based carbon molecular sieves, J. Oil Palm Res. 20 (2008) 453–460.
[30] D. Adinata, W.M.A. Wan Daud, M.K. Aroua, Preparation and characterization of activated carbon from palm shell by chemical activation with K_2CO_3, Bioresour. Technol. 98 (2007) 145–149.
[31] J.L. Figueiredo, M.F.R. Pereira, M.M.A. Freitas, J.J.M. Órfão, Modification of the surface chemistry of activated carbons, Carbon 37 (1999) 1379–1389.
[32] J. Guo, A.C. Lua, Characterization of adsorbent prepared from oil-palm shell by CO_2 activation for removal for removal of gaseous pollutants, Mater. Lett. 55 (2002) 334–339.
[33] P.J.M. Carrot, M.M.L. Ribeiro-Carrot, R.P. Lima, Preparation of activated carbon "membranes" by physical and chemical activation of cork, Carbon 37 (1999) 515–517.
[34] A.S. Mestre, J. Pires, J.M.F. Nogueira, A.P. Carvalho, Activated carbons for the adsorption of ibuprofen, Carbon 45 (2007) 1979–1988.
[35] A.A. Atia, A.M. Donia, A.M. Yousif, Comparative study on the recovery of silver(I) from aqueous solutions using different chelating resins derived from glycidyl methacrylate, J. Appl. Polym. Sci. 97 (2005) 806–812.
[36] S. Chegrouche, A. Mellah, M. Barkat, Removal of strontium from aqueous solutions by adsorption onto activated carbon: Kinetic and thermodynamic studies, Desalination 235 (2009) 306–318.
[37] U. Kumar, M. Bandyopadhyay, Sorption of cadmium from aqueous solution using pretreated rice husk, Bioresour. Technol. 97 (2006) 104–109.
[38] I. Langmuir, The adsorption of gases on plane surfaces of glass, mica and platinum, J. Am. Chem. Soc. 40 (1918) 1361–1403.
[39] H.M.F. Freundlich, Über die adsorption in lösungen [Ber die adsorption in lo sungen], Z. Phys. Chem. 57A (1906) 385–470.
[40] M.M. Dubinin, L.V. Radushkevich, Equation of the characteristic curve of activated charcoal, Chem. Zentr. 1 (1947) 875.
[41] W.D. Harkins, G. Jura, Surface of solids. XIII. A vapor adsorption method for the determination of the area of a solid without the assumption of molecular area, and the areas occupied by Nitrogen and other molecules on the surface of a solid, J. Chem. Phys. Soc. 66 (1944) 1366–1377.
[42] M.M. Dubinin, The potential theory of adsorption of gases and vapors for adsorbents with energetically non-uniform surface, Chem. Rev. 60 (1960) 235–266.
[43] S. Lagergren, Zur theorie der sogenannten adsorption gelöster stoffe, Kungliga Svenska Vetenskapsakademiens. Handlingar 24 (1898) 1–39.
[44] Y.S. Ho, G. McKay, Pseudo-second-order model for sorption processes, Process Biochem. 34 (1999) 451–465.
[45] L. Wang, J. Zhang, R. Zhao, C. Li, Y. Li, C.L. Zhang, Adsorption of basic dyes on activated carbon prepared from polygonum orientale linn: Equilibrium, kinetic and thermodynamic studies, Desalination 254 (2010) 68–74.
[46] N. Barka, M. Abdennouri, M. EL Makhfouk, Removal of methylene blue and eriochrome black T from aqueous solutions by biosorption on *Scolymus hispanicus* L: Kinetics, equilibrium and thermodynamics, J. Taiwan Inst. Chem. Eng. 42 (2011) 320–326.
[47] J.X. Lin, S.L. Zhan, M.H. Fang, X.Q. Qian, H. Yang, Adsorption of basic dye from aqueous solution onto fly ash, J. Environ. Manage. 87 (2008) 193–200.
[48] S. Chakraborty, S. De, S. DasGupta, J.K. Basu, Adsorption study for the removal of a basic dye: Experimental and modeling, Chemosphere 58 (2005) 1079–1086.